

Fracture toughness and fracture mechanisms of PBT/PC/IM blends

Part IV *Impact toughness and failure mechanisms of PBT/PC blends without impact modifier*

J. WU*, D.-M. YU

Department of Mechanical Engineering, The Hong Kong University of Science & Technology, Clear Water Bay, Kowloon, Hong Kong
E-mail: mejswu@ust.hk

Y.-W. MAI

Centre for Advanced Materials Technology, Department of Mechanical & Mechatronic Engineering (CAMT), University of Sydney, Sydney, NSW 2006, Australia

A. F. YEE

Department of Materials Science and Engineering, The University of Michigan, Ann Arbor, MI 48109, USA

In this part of the series, the impact behaviour of the PBT and PC blends without impact modifier was studied. Failure mechanism of the blends under various conditions was discussed. It was found that the key toughening process, i.e. interfacial debonding-cavitation, was disabled when the blends were subjected to impact loading. Hence, the fracture of the thick PBT/PC specimens with strong interface occurred under plane-strain condition. Their impact toughness obeys the rule of mixtures and synergistic toughening could not be achieved. When thinner specimens were tested, the fracture took place under non-plane-strain condition. But, the toughness of the blends was much lower than the value predicted by the rule of mixtures. Negative blending effect was obtained. Study on the strain rate effect suggests that under impact loading, the PC domains in the blends are subjected to an additional plastic constraint imposed by the neighboring PBT matrix, which is more rigid at a higher strain rate. Since fracture of the PC is highly sensitive to the plastic constraint at the crack-tip, the PBT imposed high plastic constraint promotes brittle fracture of the PC, leading to a deteriorated impact resistance. Evidences from TEM, SEM and OM studies support the mechanism proposed. Based on this mechanism, some suggestions on the selection of polymer components and design of microstructure for rigid-rigid polymer blends are also given. © 2000 Kluwer Academic Publishers

1. Introduction

Development of polymer blends is aimed to achieve the property combinations from each individual polymer component [1–3] and, in most cases, the property combinations cannot be obtained by any one of the polymer components alone. It is now widely accepted that in order to achieve a specific property combination, the microstructure of the polymer blends has to be tailored carefully according to the properties of each individual component. Therefore, an in-depth understanding of the mechanical, physical and chemical properties of each polymer component is essential to the design of high strength and high toughness polymer blends. Moreover, this understanding should not be restricted only to the knowledge obtained from the tests

conducted on bulk polymers, but more importantly, it should include information from each polymer component when it is in a blended state.

The deformation behavior of a polymeric material in a blended state is generally expected to be different from that observed in bulk state even at identical testing conditions. This is because the size, shape and environment of the polymer are changed drastically after blending with other polymers. Certainly, the effects of testing temperature, strain rate and composition on the deformation behavior of the blend components would also be different to the effects of the factors on their corresponding bulk polymers. Therefore, the important issue is to establish the relationship between the properties obtained from both states so that the deformation behavior

* Author to whom all correspondence should be addressed.

of a polymer in its blended state can be predicted from the information obtained in its bulk state. The latter aspect has been studied for several decades and is reasonably well understood. In principle, once the correlation is established, tough polymer blends may be designed through proper selection of polymer components, optimum composition and well-controlled microstructure. But unfortunately, the development of such a relationship is still afar despite many years of research in this field.

The purpose of this work is to investigate the effects of composition, strain rate and stress state on the impact fracture toughness of the PBT/PC blends. Special attention was focused on the mechanisms involved in the deformation processes of the blends and especially, on the significance of each component in the blended state. Possible correlation between the properties of PBT and PC in bulk and blended states was discussed with due consideration of the influence of stress state, strain rate and morphology of the blends.

2. Experimental work

A group of PBT/PC blends with different composition were employed in this study. The blends have the same composition and were made under identical processing conditions as those used in one of our earlier work [4]. The morphological details of the blends can also be found in the same paper.

Charpy impact tests were conducted on a Zwick 5102 pendulum impact tester at an impact velocity of 2.93 m/s. The single edge notched (SEN) sample geometry was adopted. Two different sample thickness was employed to investigate the effect of plastic constraint on the impact toughness of the blends. The dimensions of the specimens were $6.4 \times 12.75 \times 64 \text{ mm}^3$ and $3.2 \times 12.75 \times 64 \text{ mm}^3$, respectively. The length of the specimens for strain rate effect tests was 140 mm. All specimens were notched at the centre of one side with different notch length in order to apply the specific essential work of fracture method [5, 6].

The investigation on the strain rate effect on the fracture toughness was performed under four different strain rates, namely 23, 46, 88 and 143 s^{-1} , which were achieved by changing the test span from 40 to 100 mm. The gross strain rate (e) was calculated according to Birch and Williams [7] by $e = 6(V/W)(W/S)^2$, where V is the impact velocity, W the sample width and S the test span, respectively. The impact fracture energy was directly read from the scale on the impact tester during the tests.

Scanning electron microscope (SEM), transmission electron microscope (TEM), reflected and transmitted optical microscopes (ROM and TOM) were used to study the fracture mechanisms. The samples for SEM study were directly taken from the broken pieces after the impact tests. The fracture surfaces of the broken pieces were first covered with gold and then examined with a JOEL-35C SEM.

The ultra-thin sections containing an arrested crack tip for TEM analysis were cut using a Reichart Ultracut E ultra-microtome. The plane of the thin sections was perpendicular to the crack plane. After cutting, the

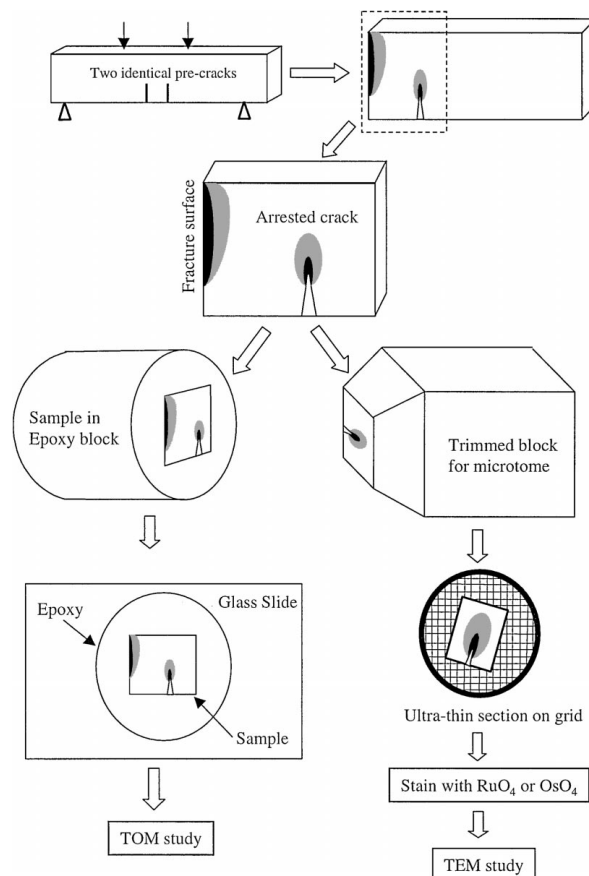


Figure 1 Schematic of TEM and TOM sampling processes.

thin sections were then mounted on copper grids and, for improved contrast, the specimens were exposed to RuO_4 vapour for 10 min. The schematic of the TEM sampling process is illustrated in Fig. 1 and more information on the TEM sample preparation can be found in Part 2 of this series [8] and elsewhere in [9]. TEM study was carried out on a Phillips CM20.

An optical microscopy (OM) study was performed on a LEITZ (LABORLUX 12 POL S) optical microscope. The OM samples approximately $10 \mu\text{m}$ in thickness were prepared using the single-edge-double-notched 4-point-bend (SEDN-4PB)/petrographic thin-sectioning technique [10]. The procedure of the OM sample preparation is also illustrated in Fig. 1. As shown in this figure, the bending bar under investigation was first double notched on one side to generate two identical pre-cracks. The notched sample was then loaded using a 4-point bend fixture. While one of the pre-cracks propagated through the entire ligament under loading, another pre-crack was arrested at subcritical condition with a damage zone at the crack tip. The half sample containing a fracture surface and the arrested crack tip was subsequently cut and embedded in an optical clear epoxy. After curing at room temperature for 8 h, one end of the epoxy cylinder was cut with a diamond saw to reveal the middle section of the deformed sample, where the highest plastic constraint was expected. The cutting plane was perpendicular to the crack surface and parallel to the specimen plane. The freshly cut surface of the cylinder was then ground and polished to a satisfactory condition before it was firmly glued on a glass slide with a cyanocrylate glue.

The epoxy block on the glass slide was subsequently mounted on the vacuum operated sample holder of a petrographic thin-sectioning system (PETRO-THIN®, Buehler) followed by cutting and grinding in the plane parallel to the surface of the glass slide. The final thickness of the sample after grinding on the thin-sectioning machine was normally less than 40 μm . After grinding the sample was finally polished on a polishing machine with different grade diamond spray (6, 3 and 1 μm) until it was completely suitable for OM observation in transmitted light. Polarized light might also be used to reveal crystalline structure and deformation patterns of the material.

3. Results and discussion

Fig. 2 shows the variation in impact fracture toughness with PBT percentage for the PBT/PC blends tested under different conditions. The effect of sample thickness on the impact toughness can be found by comparing the data obtained at 25 °C with 3.2 mm thick samples (solid circles) with those obtain at the same temperature with 6.4 mm thick samples (the unfilled squares). Similarly, the effect of testing temperature on the impact toughness can be obtained by comparison of the data obtained at 25 °C (solid circles) and -40 °C (empty diamonds) with the 3.2 mm thick samples. Three straight lines have been drawn to represent the rule of mixtures (RoM) in three cases, they are the broken line for the RoM of the fracture toughness of the PBT and PC at 25 °C with 6.4 mm thick samples; the dashed line for the RoM at -40 °C with 3.2 mm samples and the chain line for the RoM at 25 °C with 3.2 mm samples.

From the examination of the Fig. 2, it is noted that under impact condition, blending of PBT and PC at

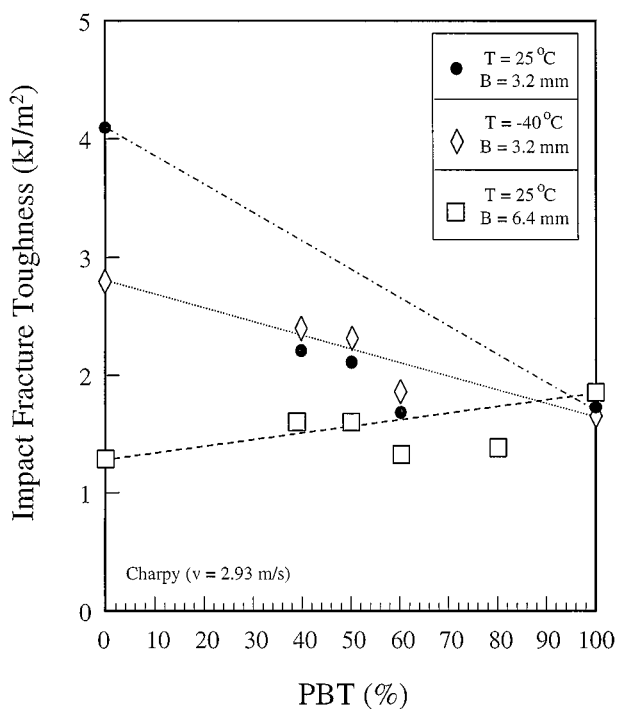


Figure 2 Variation in impact fracture toughness with PBT percentage for the PBT/PC blends obtained under various conditions.

various compositions did not introduce the anticipated toughness enhancement, that was discovered previously in the quasi-static tests [4]. In fact, blending of the two components has a negative impact on the fracture property of the polymers under high strain rate condition. For example, the impact toughness values of the PBT/PC blends obtained with 3.2 mm thick samples (solid circles) are located under the chain RoM line, indicating a negative blending effect. For the 6.4 mm thick samples, the fracture of the PC-rich blends follows the RoM. No benefit was received from blending. For those PBT-rich blends, toughness is always lower than that predicted by the RoM lines, regardless the test condition used. In general, it was failed in the present work to create a PBT/PC blend with enhanced impact fracture toughness. Since improvement in the impact property of homopolymers for particular end-application is one of the major driving forces for polymer blending, study of the mechanisms responsible for the observed negative blending effect is of theoretical and practical importance and will be pursued in the following text.

Based on the fracture mechanics theory, fracture toughness of a material depends on the volume of material capable of plastically deforming prior to fracture. This volume, in other words, the plastic zone size in front of the crack tip, depends on the stress-state acting at the crack tip. The minimum plastic zone size, hence lowest fracture toughness, is obtained under plane-strain conditions whilst large plastic zone size can be achieved when plane-stress conditions prevail. Among many other factors, sample thickness, testing temperature and deformation rate (or strain rate) are three factors, that can affect the stress-state at the crack-tip significantly. When a specimen is thick in a direction parallel to the crack front, a large stress in the thickness direction can be generated and will restrict plastic deformation in that direction, leading to high plastic constraint. For a given material, there exists a critical sample thickness, above which plane-strain condition is reached and the lowest toughness, *plane-strain fracture toughness*, is obtainable. The capacity of plastic deformation for a polymer material also changes with environment temperature. At low temperature, because of reduced polymer chain mobility, the yield stress of the polymer will be higher than that at high temperature. Therefore, smaller plastic zone size and lower fracture toughness are generally expected at lower testing temperatures. In fact, use of low temperature to obtain the plane-strain fracture toughness using thin samples is a common practice when thick sample is not available or not practical. Similar to the low temperature situation, the yield stress of a polymer material will be higher at high strain rate. This is because the relaxation of the macromolecular chain requires a relatively long time to correspond to the outside loading. At high strain rate, such as under impact, the loading time is too short for the macromolecular chains to relax. Hence, plastic deformation is suppressed by the high strain rate. Although all three factors will affect the stress-state at a crack-tip, the degree of the influence from these factors varies from material to material. Depending on

the molecular architecture of individual polymer, some may be strongly affected by sample thickness and/or temperature but others may be more sensitive to the change in strain rate.

In the present study, it is found that the fracture of the bulk PC is highly sensitive to the sample thickness and moderately to the environment temperature. As demonstrated in Fig. 2, the impact toughness of the bulk PC at 25 °C decreased from 4.12 to 1.31 kJ/m² when sample thickness was increased from 3.2 to 6.4 mm. In the quasi-static fracture tests of the bulk PC, the thickness-dependency of the fracture toughness was also found. As demonstrated in ref. [4], the quasi-static fracture toughness value of the 3.2 mm PC samples was higher than that of the 6.4 mm samples. The significant thickness sensitivity of PC fracture was also reported by Fraser and Ward [11] and Brown [12]. It was shown in [11] that the fracture energy of a bulk PC at -20 °C decreased from 3 to 1 kJ/m² when the sample thickness was increased from 2.5 to 10 mm. This finding is in agreement with our observation and suggests that the fracture of the bulk PC depends very much on the plastic constraint imposed by the sample thickness.

On the other hand, it was also noticed that the fracture of bulk PC is virtually insensitive to the strain rate within the range of the present study. The toughness values obtained in quasi-static fracture tests (at 5 mm/min or $\sim 2.45 \times 10^{-3} \text{ s}^{-1}$) and impact tests (at 2.93 m/s or $\sim 1 \times 10^2 \text{ s}^{-1}$) are essentially the same. As an example, using the 3.2 mm sample thickness at room temperature, the impact toughness is 4.12 kJ/m² (refer to Fig. 2) and the quasi-static fracture toughness was 4.10 kJ/m² (refer to [4]); with 6.4 mm samples at room temperature, the impact toughness is 1.31 kJ/m² (refer to Fig. 2) and the quasi-static fracture toughness was 1.70 kJ/m². Clearly, for a given sample thickness and temperature, fracture of bulk PC is not sensitive to strain rate. Supportive evidence to this conclusion can also be found in an early study done by Yee [13]. The author reported in the work that with 3.2 mm thick samples, the fracture of the bulk PC occurred essentially in plane-stress condition in the deformation rate range $2.54 \times 10^{-2} \text{ cm/s}$ to $2.54 \times 10^2 \text{ cm/s}$. All failures were ductile with extensive cold flow on the fracture surfaces. No noticeable strain rate effect was observed. On the other hand, all 6.4 mm thick samples would undergo brittle failure when tested under identical strain rate conditions. Yee suggested that although the fracture energy for 3.2 and 6.4 mm PC specimens were remarkably different, however, the fracture energy for a given sample thickness was virtually insensitive to deformation rate in the range studied.

Contrary to the bulk PC, the fracture of the bulk PBT is strongly influenced by the strain rate used. For instance, the quasi-static fracture toughness of the 6.4 mm thick PBT at 5 mm/min ($\sim 2.45 \times 10^{-3} \text{ s}^{-1}$) was 10.40 kJ/m² (refer to [4]), whilst the impact toughness of the very same PBT sample at 2.93 m/s ($\sim 1 \times 10^2 \text{ s}^{-1}$) is only 1.85 kJ/m², see Fig. 2. Similar strain rate-dependency of PBT fracture was also reported in a previous work [14] by Hobbs and Bopp. The critical stress intensity factor, K_{IC} , of a bulk PBT sample was

found to drop from 6.59 to 3.08 MPa√m when the deformation rate was changed from 5 mm/min ($\sim 2 \times 10^{-1} \text{ in./min}$) to 2.93 m/s ($\sim 6.92 \times 10^3 \text{ in./min}$), showing a significant strain rate effect.

Regarding to the sample thickness effect, the fracture of the bulk PBT is, once again, opposite to the bulk PC. It is not sensitive to sample thickness and testing temperature in high strain rate impact tests. As shown in Fig. 2, the impact toughness of the bulk PBT is around 1.85 kJ/m², regardless of sample thickness and test temperature used.

Based on the above discussion, we may summarize that the stress-state at the crack-tip in the bulk PC is highly sensitive to the sample thickness change, i.e. depends critically on the degree of plastic constraint imposed by sample geometry. When the PC is thin and under the plane-stress condition, fracture toughness will be high and not sensitive to the strain rate. But, when the PC is subjected to the plane-strain condition, brittle fracture occurs even under quasi-static loading. In general, fracture toughness of the PC will decrease with increase of the plastic constraint at the crack-tip. On the other hand, PBT is more sensitive to strain rate. Deformation behaviour of bulk PBT varies with applied strain rate significantly. Although ductile fracture occurs under quasi-static loading, it becomes more rigid and brittle under high strain rate impact loading. Impact toughness of the PBT is always low and not very sensitive to sample geometry and environment temperature.

Given the above mentioned fracture characteristics of the PC and PBT, the failure mechanisms behind the negative effect of the PBT/PC blending may be proposed as following. In a previous paper of this series [4], we discovered that the PBT/PC (40/60) and (50/50) blends have a bi-continuous structure. The PC phase forms a continuous network penetrating through the PBT matrix. Both TEM and SEM micrographs showed that the interfacial bonding between the PBT and PC is quite strong due to the compatibilization effect of the PBT/PC copolymers generated during mixing via transesterification. When the fracture of the blends takes place under quasi-static loading, direct TEM evidence suggested that debonding-cavitation at the PBT/PC interface occurs prior to fracture and, because of this debonding-cavitation, the plastic constraint in sample thickness direction is greatly reduced. As a result, the stress-state at the crack-tip is converted from plane-strain condition to plane-stress condition. Under the plane-stress condition, the very thin PC domains in front of the crack-tip are ductile and capable of bridging the propagating crack and absorbing large amount fracture energy through plastic deformation. Through this mechanism, quasi-static fracture toughness of the blends is improved. Obviously, for this toughening mechanisms to happen, the key is the occurrence of the debonding-cavitation process before fracture.

Microscopic study of the debonding-cavitation suggests that the interfacial debonding process should consist of three steps, namely, initiation of a craze-like structure at the interface, growth and breakdown of the craze-like structure. It is evident that the whole process will take some time to complete. Under quasi-static

loading, this should not be a problem since loading time is long in quasi-static case. But, under high strain rate impact condition, the debonding process may not have sufficient time to complete due to very short loading time. This is particularly true when the debonding process involves relaxation of rigid polymer chains.

In the present study, as both PBT and PC are rigid polymers, one would therefore expect that the time needed for debonding at the PBT/PC interface is longer, or much longer, than the impact loading time. Hence, the debonding-cavitation is unable to complete and the stress-state at the crack-tip would remain in the plane-strain condition. If there is no other event to relieve the plane-strain condition, the PC domains will undergo brittle fracture because, as mentioned before, the plane strain fracture toughness of the PC is low. Since the impact fracture toughness of the PBT is intrinsically low, the toughness of the PBT/PC (40/60 and 50/50) blends under this situation should be no higher than the value predicted by the RoM of the plane-strain toughness of the bulk PC and PBT. This prediction has been proven to be correct for the 6.4 mm thick samples of the 40/60 and 50/50 blends. As shown in Fig. 2, the two empty squares representing the 40/50 and 50/50 blends are located on the broken RoM line.

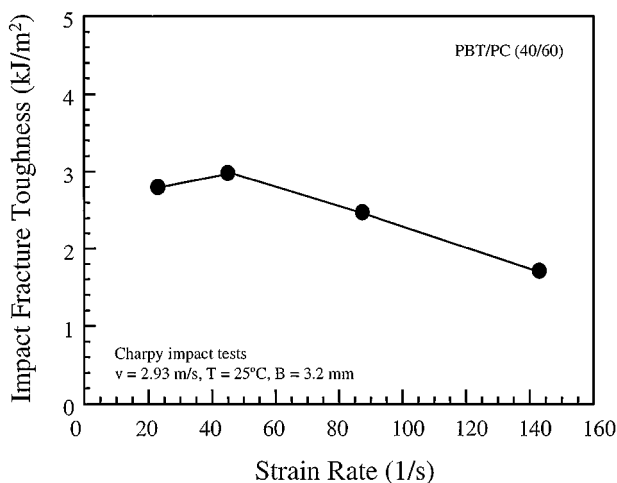
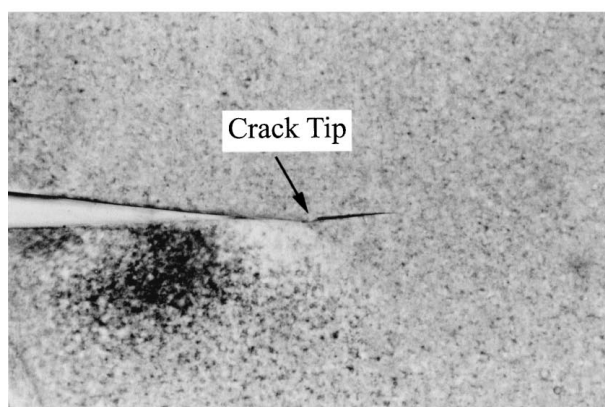
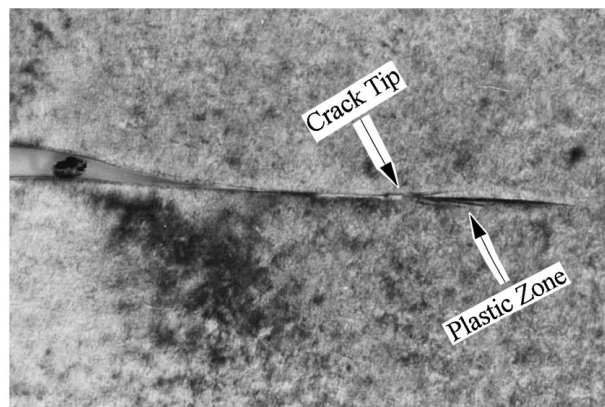


Figure 3 Variation in impact fracture toughness with strain rate at 25 °C for the PBT/PC (40/60) blend, sample thickness is 3.2 mm.



(a)



(b)

Figure 4 TOM micrographs of arrested crack-tips obtained with the PBT/PC (40/60) at (a) high strain rate (143 s⁻¹) and (b) relative low strain rate (23 s⁻¹) (visual magnification; ×25).

For the thinner 3.2 mm samples of the 40/60 and 50/50 blends, the toughness values of the blends fall on the dash RoM line of the PBT and PC obtained at -40 °C. They are higher than that predicted by the broken RoM line for the 6.4 mm samples, but lower than that predicted by the chain RoM line, which is the RoM of the plane-strain toughness of the PBT and non-plane-strain toughness of the PC. The implication of this phenomenon is that the degree of the plastic constraint on the PC domains inside the 3.2 mm blends is actually higher than the constraint level expected for 3.2 mm bulk samples. The fracture toughness of the PC domains in the 3.2 mm blends at 25 °C is somehow close to the fracture toughness of the 3.2 mm bulk PC at -40 °C. It seems that the PC domains of the blends are subjected to additional plastic constraint, that further embrittles the PC domains.

To disclose the causes behind the additional plastic constraint, we may recall that the rigidity and deformation of the PBT is strongly influenced by the strain rate. The rigidity increases and toughness decreases with the strain rate increase. Therefore, when the blends are subjected to high strain rate loading, though the thin PC domains intrinsically are able to elongate in the principal stress direction and shrink laterally, the neighboring PBT matrix becomes more rigid at the high strain rate and the deformation of the PBT matrix is suppressed. Since the adhesion of the PBT/PC interface is high and debonding-cavitation does not have sufficient time to take place, lateral contraction of the PC domains are stopped by the rigid PBT matrix, i.e. the PC domains are now subjected to an additional plastic constraint imposed by the rigid neighboring PBT matrix. This is somewhat similar to the situation of a thin adhesive layer sandwiched between two rigid adherents in which the toughness of the adhesive is reduced below that of bulk adhesive material [15].

To confirm this strain rate induced embrittlement, impact fracture toughness of the 40/60 blend was tested at various strain rates using 3.2 mm thick specimens. The results of the tests are shown in Fig. 3. Evidently, with increasing impact strain rate, the fracture toughness of the PBT/PC (40/60) blend decreases from ~3 to 1.34 kJ/m², indicating that plastic constraint is higher

at higher strain rate. TOM study shows that the lower toughness at higher strain rate is mainly caused by the reduced plastic deformation. Fig. 4a and b are the TOM photographs taken from the arrested crack tips obtained under two strain rates. They clearly illustrate that the crack tip obtained at a higher strain rate (143 s^{-1}) is sharp and no noticeable plastic deformation is seen at the crack-tip, see Fig. 4a. However, at a lower strain rate (23 s^{-1}) there is a limited plastic zone in front of the tip, see Fig. 4b. Further evidence from TOM

study shows that fracture surfaces is relatively smooth at higher strain rate (Fig. 5a) and much coarser at lower strain rate (Fig. 5c). A plastically deformed zone, black in colour and with crack branches, has been found underneath the fracture surface at low strain rate, Fig. 5d. The fracture surface at high strain rate shows no such features, Fig. 5b.

SEM micrographs taken from the crack initiation area of the fracture surfaces obtained at different strain rates confirm the conclusions drawn from the above

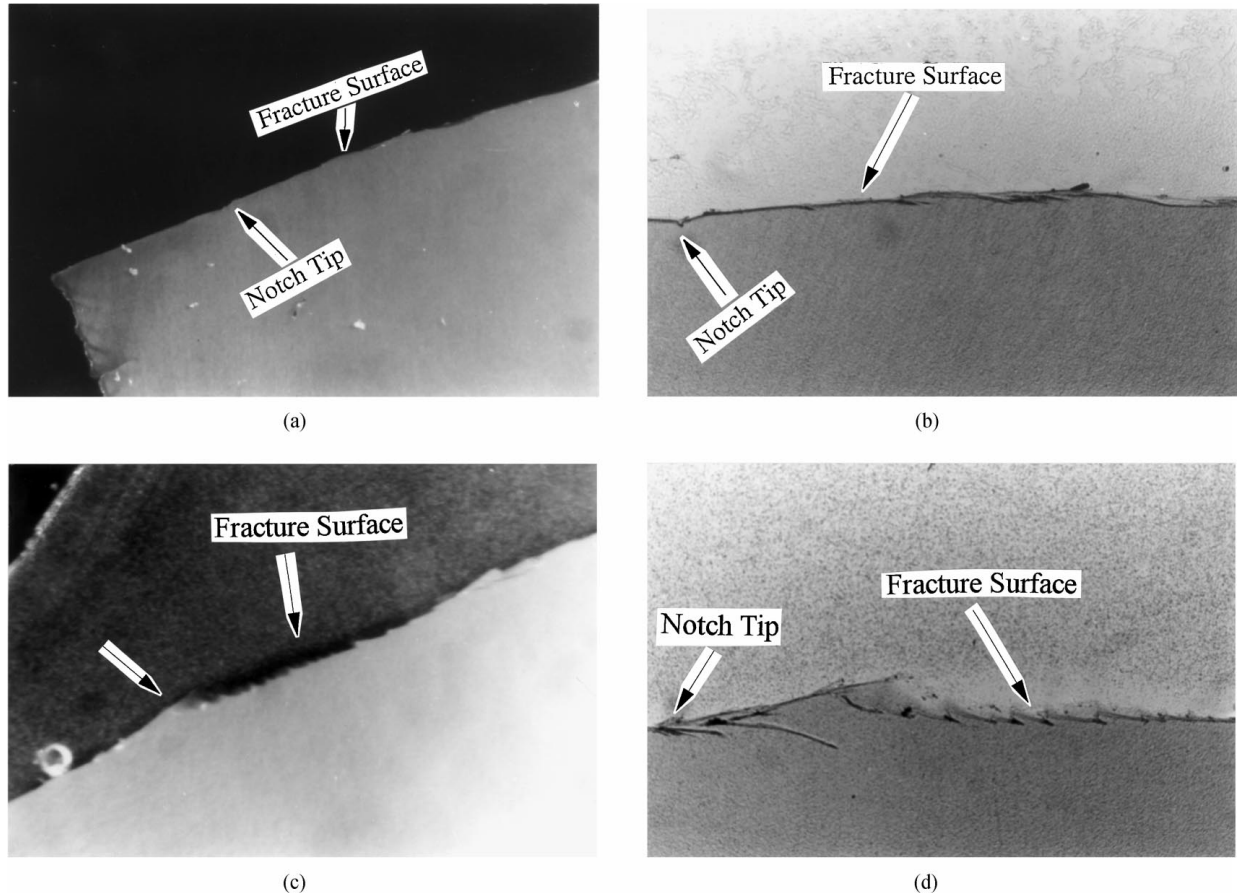


Figure 5 (a) Side view in polarized light of the fracture surface of the PBT/PC (40/60) blend impact fractured at high strain rate (143 s^{-1}). (visual magnification; $\times 75$); (b) View in reflect light of the zone underneath the fracture surface of the PBT/PC (40/60) blend impact fractured at high strain rate (143 s^{-1}). (visual magnification; $\times 250$); (c) Side view in polarized light of the fracture surface of the PBT/PC (40/60) blend impact fractured at relative low strain rate (23 s^{-1}). (visual magnification; $\times 75$); (d) View in reflect light of the zone underneath the fracture surface of the PBT/PC (40/60) blend impact fractured at relative low strain rate (23 s^{-1}). (visual magnification; $\times 250$).

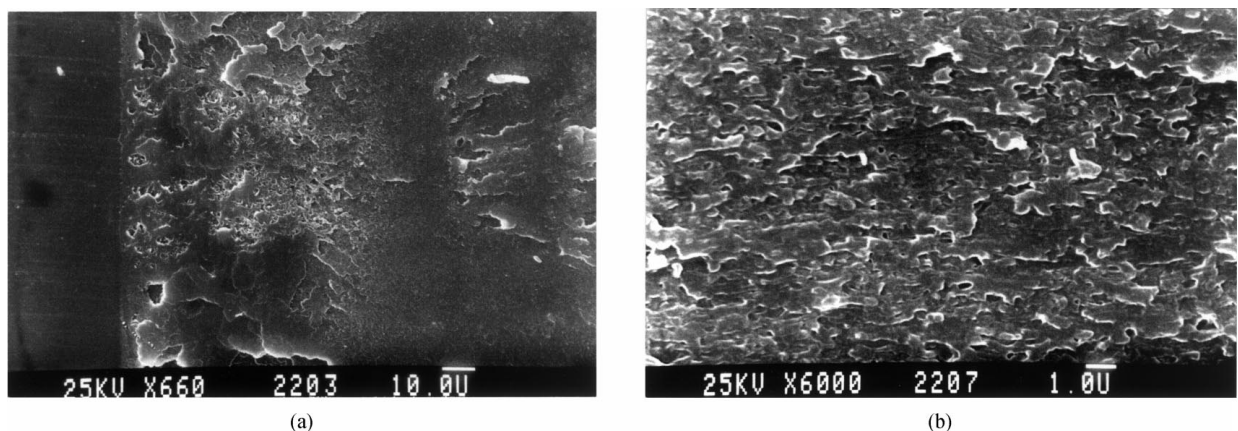
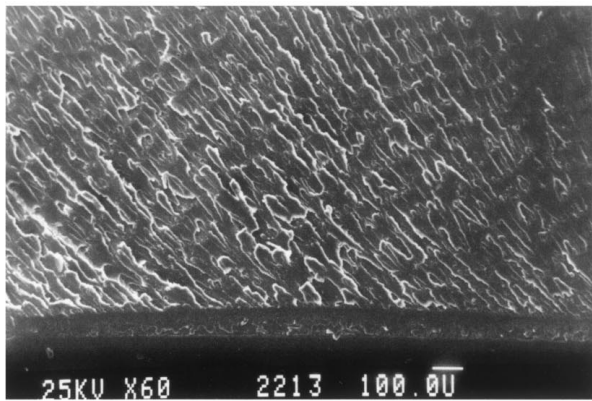
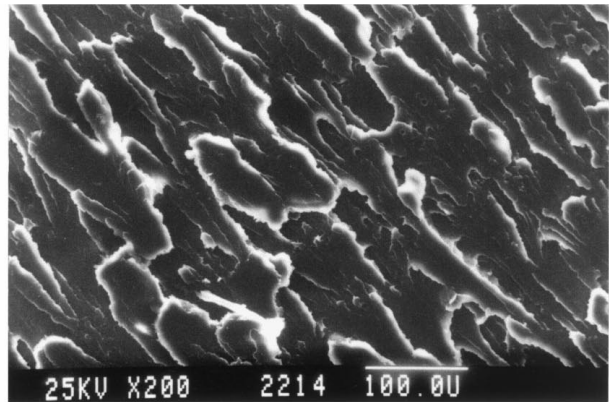


Figure 6 (a) SEM micrograph of the fracture surface of the PBT/PC (40/60) blend impact fractured at high strain rate (143 s^{-1}); (b) Enlarged SEM micrograph of the fracture surface near the crack initiation area of the PBT/PC (40/60) blend impact fractured at high strain rate (143 s^{-1}).

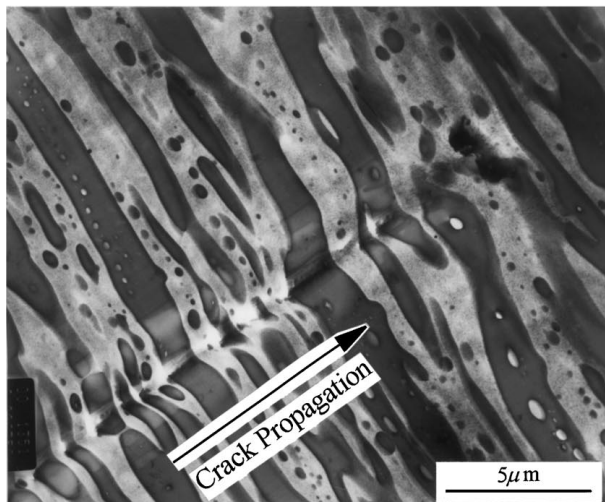


(a)

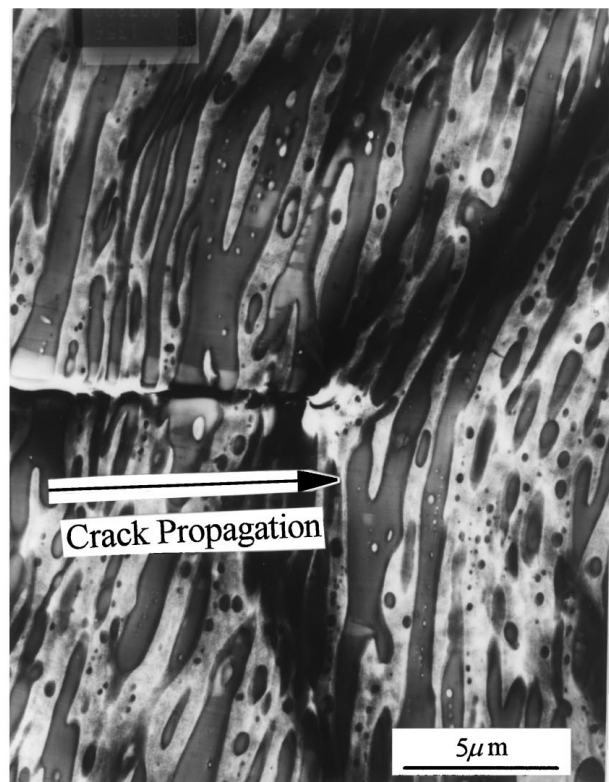


(b)

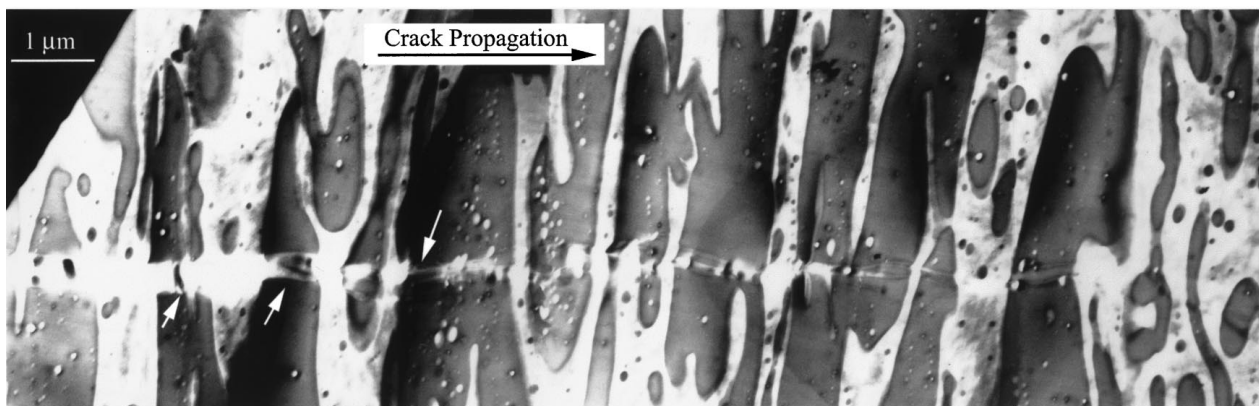
Figure 7 (a) SEM micrograph of the fracture surface of the PBT/PC (40/60) blend impact fractured at relative low strain rate (23 s^{-1}); (b) Enlarged SEM micrograph of the fracture surface near the crack initiation area of the PBT/PC (40/60) blend impact fractured at relative low strain rate (23 s^{-1}).



(a)



(b)



(c)

Figure 8 (a) and (b) TEM micrographs taken from the arrested crack-tips of the PBT/PC (40/60) blend impact fractured at high strain rate (143 s^{-1}); (c) TEM micrographs taken from the arrested crack-tip of the PBT/PC (40/60) blend impact fractured at relative low strain rate (23 s^{-1}).

analysis. As can be seen, all the SEM micrographs (Figs 6a and b and 7a–c) show that the interfacial bonding of the blend is good and no sign of debonding is sighted. Fig. 6a and b are the SEM micrographs taken from the high strain rate fracture surface. Less plastic deformation and smoother surface are evident, as compared to the SEM micrographs taken from the low strain rate fracture surface in Fig. 7a and b. Coarse fracture surface consisting of highly stress whitened materials are clearly seen in Fig. 7b.

Our TEM study on the failure mechanisms of the blends also lends support to the above interpretation. A TEM micrograph taken from an arrested crack tip obtained at high strain rate shows that the growing crack tip is sharp, refer to Fig. 8a and b. Both PC and PBT domains fractured in a brittle manner. Neither debonding at interface nor large scale plastic deformation of either PC or PBT can be seen, indicating that the materials were under high plastic constraint during the fracture. At relatively low strain rate, the TEM micrograph of the arrested crack-tip displays some PC domain plastic deformation and bridging in a very limited degree, as indicated by the arrows in Fig. 8c. But, brittle fracture of both the PBT and PC occurred in general.

For the two PBT-rich blends, i.e. PBT/PC (60/40) and (80/20), negative blending effect on toughening is always found and the toughness values of these two blends are below the corresponding RoM line. The causes of the negative blending effect are not difficult to understand. Since the PBT-rich blends consist of dispersed PC particles in the continuous PBT matrix and the interfacial bonding between the PBT and PC is very poor [4], when a cracked sample is loaded, the PC particles are unable to share the applied stresses with the PBT matrix. Instead, they will act as stress concentrators and promote the crack propagating. Moreover, the poor PBT/PC interfaces are pre-existing surfaces, which make no contribution to energy dissipation. New fracture surfaces are only generated through the fracture of the PBT matrix. Therefore, the actually area of the new fracture surface is significantly smaller than the cross-section area of the specimens. This also leads to a lower calculated toughness value than that predicted by the rule of mixtures.

4. Summary

Improvement of impact toughness by blending PBT and PC without rubbery impact modifiers was attempted, but failed. The possible failure mechanisms are proposed based on fracture mechanics theory, fracture characteristics of the bulk PBT and PC, morphology structure of the blends and the deformation behaviour of the PBT and PC in blended state. The key points of the failure mechanism are summarized in the following.

For the PBT-rich blends, PBT/PC (60/40) and (80/20), the negative blending effect on toughening is stemmed from the very poor interfacial adhesion between the two phases. The PC phase in this situation is non-load bearing and provides the propagating crack with an easy path. The PBT/PC interfaces reduce the effective fracture surface area as well.

For the PC-rich blends, the failure is a result of combined factors, including the fracture characteristics of the PBT and PC, interfacial bonding condition and applied load. Briefly, the PBT matrix becomes more rigid under high strain rate loading and will impose a higher plastic constraint on the PC domains, if the interfacial bonding between the PBT and PC is strong. This high plastic constraint will maintain the stress-state at the crack-tip in a plane-strain dominant condition. If debonding-cavitation occurs prior to fracture, the plane-strain condition will be converted to the plane stress condition. However, if it fails to occur due to short loading time, such as in impact case, the high plastic constraint will promote brittle fracture of the PC domains, because the fracture of the PC is highly sensitive to the degree of plastic constraint. The overall fracture of the specimen will take place in brittle mode, leading to reduced fracture toughness.

Strong experimental evidences supportive to this failure mechanism were obtained in OM, SEM and TEM investigations as well as in the toughness-strain rate relationship test.

Some suggestions on the selection of polymer components and structure design for new rigid-rigid polymer blends may be proposed here based on the results of the present study. To improve the impact fracture toughness of the rigid-rigid polymer blends, the strain rate sensitive PBT component may be replaced by a less strain rate sensitive polymer component. Alternatively, on a more practically level, a very small amount of rubbery particles may be added into the PBT phase, rather than in the PC phase, in order to reduce its strain rate sensitivity of the PBT. Introduction of rubbery particles into the PC phase may eliminate the crack bridging effect of the PC domains, as the yield strength of the PC will be heavily decreased by the rubbery particles. Lastly, use of small amount of soft chain copolymers to form the PBT/PC interface. The soft chain copolymer interface should be able to debond readily at impact loading.

Some of the suggestions have been attempted in our lab. The results will be reported in the successive part of this series.

Acknowledgement

J. S. Wu wishes to thank the Hong Kong Research Council for the financial support to the current project (HKUST810/96E). Y.-W. Mai wishes to acknowledge the Australian Research Council (ARC) for the continuing support of the polymer blends projects. Authors are grateful to the Advanced Engineering Materials Facility (AEMF) and the Materials Characterization and Preparation Facility (MCPF) of the Hong Kong University of Science and Technology for the assistance in use of their facilities. The donation of the PBT and PC by G E Plastics and the Dow Chemical Co. is greatly appreciated.

References

1. D. R. PAUL and J. W. BARLOW, *J. Macromol. Sci.-Rev. Macromol. Chem.* **c18**(1) (1980) 109.

2. D. R. PAUL and S. NEWMAN, "Polymer Blends," Vol. 1 (Academic Press, New York, San Francisco, London, 1978).
3. *Idem.*, *ibid.* Vol. 2 (Academic Press, New York, San Francisco, London, 1978).
4. J. S. WU, A. F. YEE and Y.-W. MAI, *J. Mater. Sci.* **29** (1994) 4510.
5. Y. W. MAI, *Int. J. Mech. Sci.* **35** (1993) 995.
6. J. S. WU, Y.-W. MAI and B. COTTERELL, *J. Mater. Sci.* **28** (1993) 3373.
7. M. W. BIRCH and J. G. WILLIAMS, *Int. J. Fract.* **14** (1978) 69.
8. J. S. WU and Y.-W. MAI, *J. Mater. Sci.* **28** (1993) 6167.
9. H. SUE, *Polym. Eng. and Sci.* **31** (1991) 275.
10. M. T. TAKEMORI and A. F. YEE, in "Impact Fracture of Polymers—Materials Science and Testing Techniques," edited by K. Takahashi and A. F. Yee (Kyushu University, Fukuoka-shi, Japan, 1992) pp. 331–392.
11. R. A. W. FRASER and I. M. WARD, *Polymer* **19** (1978) 220.
12. H. R. BROWN, *J. Mater. Sci.* **17** (1982) 469.
13. A. F. YEE, *ibid.* **12** (1977) 757.
14. S. Y. HOBBS and R. C. BOPP, *Polymer* **21** (1980) 559.
15. H. R. DAGHYANI, L. YE and Y.-W. MAI, *J. Adhesion* **53** (1995) 149.

*Received 9 February
and accepted 12 July 1999*